6th World Congresses of Structural and Multidisciplinary Optimization
Rio de Janeiro, 30 May - 03 June 2005, Brazil

Additional Strength of Prefabricated Piles Due to Dynamic Instability During Driving Process

Reyolando Manoel Lopes Rebello da Fonseca Brasil(1), Marcelo A. Silva(2), Urbano R. Alonso(3) and Valmir Merighi(4)

(1) - Department of Structural and Foundations Engineering of Polytechnic School of The University of Sao Paulo, PEF/EPUSP – Associated Professor
Cx. Postal 61548, CEP 05.424-970, Sao Paulo -SP., Brazil
E-mail: rmlrdfbr@usp.br

(2) - Department of Structural and Foundations Engineering of Polytechnic School of The University of Sao Paulo, PEF/EPUSP – Pos-Doctoral Researcher
E-mail: m_araujo_silva@uol.com.br
- Scac Fundações e Estruturas Ltda., Structural Technical Division – Project Manager

(3) - Urbano Alonso Consultoria e Projetos Ltda.
- Ex-Professor of Mackenzie and FAAP, E-mail: u.rodriguez@uol.com.br

(4) - Department of Structural and Foundations Engineering of Polytechnic School of The University of Sao Paulo, PEF/EPUSP – Master Student
- Scac Fundações e Estruturas Ltda., Foundation Technical Division – Technical Manager
E-mail: eng.fundacoes@scac.com.br

Abstract
Slender reinforced concrete prefabricated piles (relationship length/diameter> 30) are subject to imposed displacements when driven through thick layers of submerged soft clay. Those displacements are due to a phenomenon of random directional dynamic instability that takes place during the driving process. In the present paper, the authors present results of researches carried out to determine the strength of piles subjected to those imposed displacements. A real case of a SCAC prefabricated pile, driven in Santos-SP., Brazil, was analyzed. That pile was part of a universe of 624 driven piles, for which six static load tests were done. To analyze the pile behavior under those imposed displacements, the authors discretized the pile in beam finite elements. The material nonlinear behavior of the cross-sections was given by the effective stiffness concept based on Optimization techniques applied to experimental results. Bending tests were carried out at SCAC plant in São Paulo in similar piles to determine the effective stiffness, as function of the bending moment level. In those tests, the structural failure loads were also measured. The soil that involves the driven piles was modeled as springs with perfect elastoplastic behavior (Winkler´s model). Surveys of the soil were used for the determination of the spring constants and the soil failure stresses. The imposed displacements were the loading considered. Due to the nonlinear behavior considered in the structural model, an iterative process was used to carry out the structural analysis. After the model solution, the strengths were computed precisely. It was observed from the results that the strengths are significant and their values are around the same value of Brazilian Code based ultimate bending moment and inferior to the real failure bending moment, obtained in tests. It was verified, in the present research, that the centrifuged reinforced concrete pile, fabricated by SCAC, resists satisfactorily. Static load tests were accomplished and they showed that the driven piles resisted to the loads considered in the original design of the foundation and to the additional loads due to the phenomenon of random directional dynamic instability and that they comply to the pertinent Codes.

Key words: Structural optimization; reinforced concrete; dynamic instability; driven piles.

1. Introduction

Slender pre-cast concrete piles driven through submerged very soft to soft clay, usually undergo large curvatures due to random dynamic instability phenomena during the driving process. After a driver hammer blow, a pile will vibrate around a equilibrium configuration. When the next blow is delivered, the pile will be in a position very hard to determine due to the problem's several random variables. The blow delivered to a pile's deformed configuration will force it to a random curved position. The same phenomenon will repeat itself for the next blows, resulting significant random pile displacements.

Brazilian code NBR-6122-96 **[7]** establishes bounds to the pile verticality, that are usually respected in the first meters under the surface. After that, in thick soft clay layers, the piles will undergo random behavior in spite of the efforts of the driving crew. As a matter of fact, two piles side by side, in the same soil, may present quite different configurations after driving. Measuring and considering those displacements have very rarely being done and reported in current literature. Figure 1 shows the deformed configurations of two piles made by SCAC, 50 *cm* diameter, driven in the Santos, Brazil, region, whose displacements were reported by Aoki and Alonso **[3]**. The black vertical lines represent the prescribed positions, while the pink curved lines display the measured final positions of the piles after the driving process. Some of the measured displacement values are shown. In the present paper, only the critical case, of A pile, is considered.

One of the chief concerns of this problem is to determine what are the additional stresses in the piles in a such a case, as they are directly related to the displacements and to both the pile and soil stiffness. This latter stiffness is determinate as function of the underground survey and modeled as springs attached to the structure. The material nonlinear behavior of the cross-sections was given by the effective stiffness concept (Silva and Brasil **[14, 15]** and Brasil and Silva **[9, 10]**), based on optimization techniques applied to experimental results.

As a byproduct of our research, we intend to provide an Engineering tool to determine internal stresses in piles driven through very soft soils.

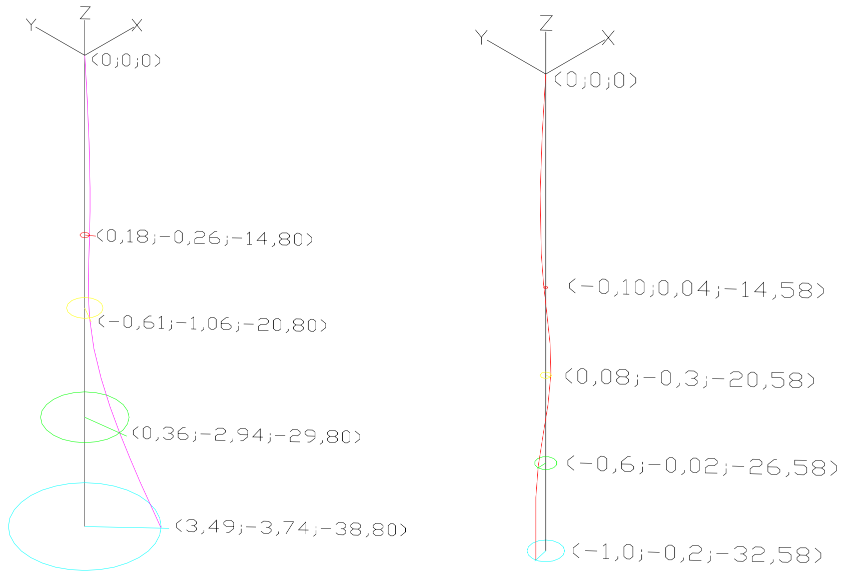

Figure 1 – Final shape of pile manufactured by SCAC, 50 cm diameter, driven in Santos region, Brazil, reported by Aoki and Alonso **[3]**

2. Literature review

In the present paper we approach several engineering issues such as soil-structure interaction, nonlinear structural analysis, reinforced concrete and optimization. In this section we present resumed reference to our main sources.

As we already mentioned, Aoki and Alonso **[3]** performed measurements of the lateral displacements due to random directional dynamic instability in two piles manufactured by SCAC, driven in the Santos region, Brazil. They concluded that the phenomenon may lead to severe curvatures of the pile axis. Thus, dynamic stresses during the driving process and the static stresses under service loading, both in the concrete and the connection devices, will be larger than predicted for the straight case. It is of fundamental importance that those elements should resist to those extra stresses. In the case of the mentioned construction in the Santos region, Brazil, where 624 piles were driven and 6 static load proofs were performed, the authors concluded:

a) SCAC piles supported the dynamic stresses during the driving process and presented a larger than 2 safety ratios in the static load proofs;

b) the 1:100 angular maximum deviation prescribed by NBR-6122-96 **[7]** Brazilian code will apparently apply to piles with *L*/*D* relationship less than 30.

The soil stiffness and bearing characteristics were estimated from obtained local underground survey. In the case, Winkler's model was used (Alonso **[2]**).

Reinforced concrete concepts follow references Sussekind **[16]**, Fusco **[12]**, Santos **[13]** and NBR-6118-03 **[6]** Brazilian code. For reinforced concrete beams the bending stiffness, as it is obvious, depends on the value of the bending moment, as well as the component material proprieties and the reinforcement position. An empirical formula proposed by D. E. Branson in 1963, to determine a section effective stiffness, was incorporated by ACI-318-71 **[1]** and also by NBR-6118-03 **[6]** Brazilian code. Recently Silva and Brasil **[14, 15]** and Brasil and Silva **[9, 10]** proposed equations for the bending stiffness o a certain reinforced concrete section as function of the bending moment value. The authors presented results of experiments performed in slender structures 15, 20, 30 and 40 *m* long. Optimization algorithms were used to determine bending effective stiffness for several loading hypothesis. They minimized the error between displacements experimentally measured and those determined by an approximated numerical model. Maximum and minimal stiffness values were imposed. The determined equations relating bending stiffness to bending moment value intend to model the reinforced concrete material nonlinearity.

As for the optimization techniques, we use the Augmented Lagrangian Method (Chahande and Arora **[11]**). In our case, the stiffness of selected transverse sections are the design variables of the minimization problem of the approximation error between the experimentally measured displacements and those predicted by the adopted mathematical model. We transform this optimization problem with restrictions into a optimization problem without restrictions by creating the Augmented Lagrangian functional. The restriction functions associated to the Lagrange multipliers and the penalty parameters are combined in a objective function to obtain the Lagrangian functional. A sequence of Lagrangians is developed by appropriately varying the multiplies and penalty parameters. The minimum value of the Lagrangian functional in this sequence converges to the minimum value of the original problem. The search algorithms used in the process require that the objective functions and restrictions are differentiable with respect to the design variables. That is the so called Sensibility Analysis that uses up most of the computational time. We used the Finite Difference Method as in Arora **[4]**.

3. Computational Modeling of the Problem

3.1 Soil Modeling

We intend to determine stresses due to transverse displacements of the axis of slender pre-cast reinforced concrete piles driven into thick layers of soft clay. If we consider the value of the displacements shown in Figure 1A, we must realize that they are very large, much more so than what is allowed by NBR 6122-96 **[7]** Brazilian Code. All related data will be found in Aoki and Alonso **[3]**. We used the Finite Element Method to model the pile and the surrounding soil. The latter was modeled as elastoplastic springs, as prescribed by Winkler's Model (Figure 2).

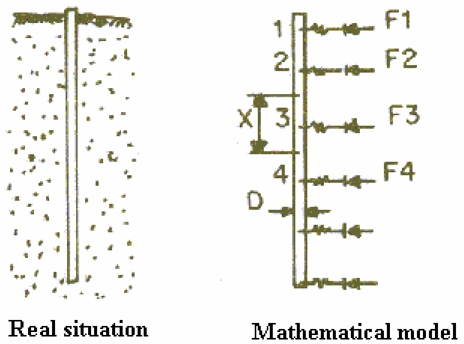

Figure 2 –Winkler´s Model

In this model, the surrounding soil is replaced by springs attached to the nodes of the structural numerical model. The stiffness of each spring is a function of the influence area of each node and of the reaction coefficient of the soil at that level. It was computed as prescribed by (Alonso **[2]**):

$$k_z = \eta_h \frac{z}{D}, \tag{1}$$

where η_h is the horizontal reaction coefficient of the soil, D the diameter of the pile, and z the vertical coordinate of the considered node. For the model displayed in Fig. 2 validity, the tip reaction is neglected, the so called long pile hypothesis. Its length must be larger than $4T$, with

$$T = \sqrt[5]{\frac{EI_{ef}}{\eta_h}}, \tag{2}$$

where E is the concrete linear Yong's modulus and I_{ef} is the effective moment of inertia of pile section. If A_i is the influence area of the i-th node, the stiffness of the two orthogonal horizontal springs in that node are:

$$k_i = k_z A_i. \tag{3}$$

k_z is only computed up to $z = 4T$, as displacements and stresses bellow that level may be neglected. We have considered neither vertical springs along the pile nor in its tip to equilibrate transverse loading. For vertical loads, one vertical spring is provided with stiffness equal to

$$k = 200 \times N \times A \ (tf/m), \tag{4}$$

N being the resistance of the soil at the pile tip level measured in a SPT test, and A being the area of pile tip (m^2), computed inside its outer perimeter.

We adopted the rupture stress of the clay as

$$\sigma_r = 9c\,, \tag{5}$$

where c is the clay cohesion. For sand layers the rupture stress of the soil is adopted equal to

$$\sigma_r = \frac{N}{1{,}5} \;\; (kgf/cm^2). \tag{6}$$

3.2 Experiments and Analyses to Determine Bending Stiffness of the Pile

Several experiments were carried out at SCAC, Jaguaré (SP), Brazil, plant. In this case, a 50 *cm* diameter SCAC standard centrifuged concrete pile14.8 *m* long was tested. As all design characteristics of this pile are fully known, an adequate planing of the experiment was possible. We intended to evaluate the performance of the pile under both service and ultimate states. We measured the following data: applied load, displacements at prescribed sections, occurrence and width of cracks and residual displacements after unloading. The experiment was carried out with the pile n horizontal position as shown in Fig. 3. Loads were applied at transverse direction to the original pile axis, 20 *cm* bellow its tip. As a reference, a steel wire was stretched along the virtual axis and fixed to appropriated devices in such way as not to move during the experiment. Displacements were measured at MF points, shown in Fig. 3, each at least 1*m* away from the other. Two movable supports were placed under the pile, as shown in Fig. 4, to avoid bending due to gravity and friction with the soil.

The clamping device was designed to support loads 3 times larger than the predicted rupture load of the pile. As it is obvious, the transverse load applied to the tip of the pile leads to bending moments and shear forces along its length. Dynamometers and other equipment used in the experiment were dully checked by independent consultants controlled by Brazilian government authority INMETRO.

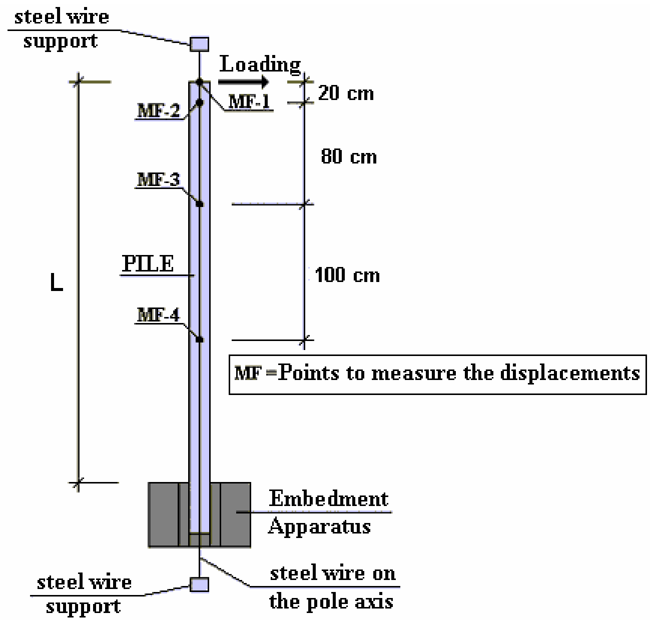

Figure 3 – Experimental set up

After the pile and measuring equipment were mounted in their proper positions, the loads were applied as shown in Fig. 3. Their value was increased in steps and after stabilization in each step the searched for parameters were measured. The first step was only 5% of the final rupture load, gradually increasing to the destruction of the specimen.

As already referred, studies on the determination of the bending stiffness of slender reinforced concrete structures as function of the bending moment value were carried out by Silva and Brasil **[14, 15]** and Brasil and Silva **[9, 10]**. We present an abstract of the procedures in Annex 1 of this paper. The effective stiffness is defined as:

$$I_{EF}(z_i) = w_i\, I(z_i), \tag{7}$$

where $I(z_i)$ is moment of inertia of the section z_i , considered as unstressed, and w_i is a effective stiffness parameter, that is, the fraction of value $I(z_i)$ that is active at that bending moment value. The full bending stiffness product is, by definition, $EI(z_i)$, while the effective bending stiffness is $EI_{EF}(z_i)$. In this paper we use the following fitted function for the effective stiffness parameter:

$$w = -0{,}209974x + 0{,}279928\,, \tag{8}$$

with

$$x = \frac{M_k}{M_u}, \qquad (9)$$

where M_k is the characteristic acting bending moment, and M_u is the section ultimate limit bending moment as predicted by NBR-6118-03 **[6]** Brazilian Code.

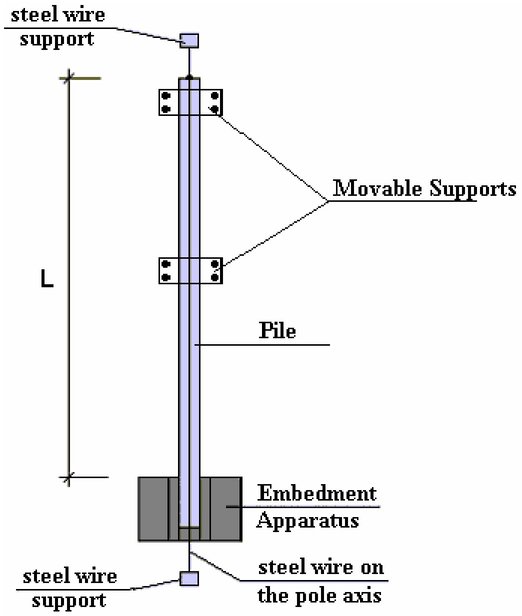

Figure 4 – Hinged movable supports for the pile

3.3 Iterative Nonlinear Structural Analysis

Back to the pile shown in Fig. 1, the subject of this paper, nonlinear behavior is due to the effective stiffness consideration. The pile and the soil are discretized resulting a node at each 1 *m* at least. We already know the real displacements, measured at the site of the pile driving. We start adopting a initial value for variable x in Eqs. (8) and (7) to obtain $I_{ef} = w(x)\ I$, the value of moment of inertia to be used in the FEM software. The program will give us a set of values for the bending moments along the structure. The largest of them will be called M_{fem}.

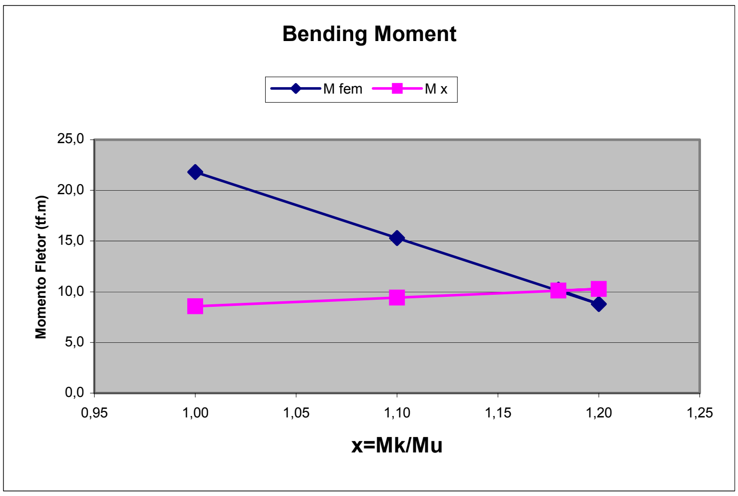

Figure 5 – Bending moments obtained via the iterative procedure at the section that presented the biggest value of bending moment

In the other hand, substituting x into (9) we compute $M_k = x\ M_u$. The ultimate limit bending moment M_u is given by NBR-6118-03 **[6]** Brazilian Code, as a function of the geometry of the section and characteristics of the steel and concrete used in the manufacture of the pile. This M_k value will be called M_x.

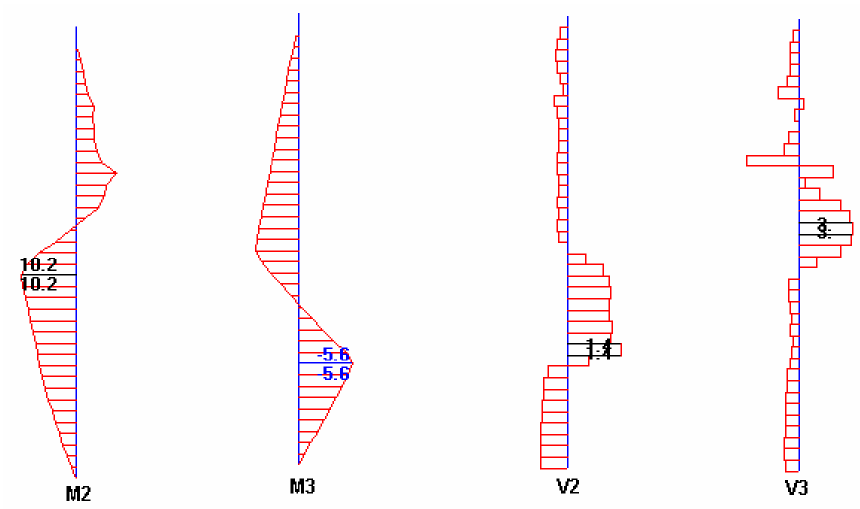

Figure 6 – Obtained bending moments

In general, for a given initially adopted x value, M_{fem} and M_x will not be the same. Thus a iterative procedure will be necessary to converge to $M_{fem} = M_x$. Thus, we can pose the following optimization problem: determine $x \in \Re$ to minimize function

$$f(x) = \frac{1}{2}\left(M_{fem}(x) - M_x(x)\right)^2 \cdot \tag{10}$$

This minimum value will be attained when $M_{fem} = M_x$. To that end, we use unconstrained optimization methods (Arora, 1989).

Table 1 – Bending moments for each iteration

k	x	M fem (tf.m)	M x (tf.m)
0	1,0	21,8	8,6
1	1,1	15,3	9,4
2	1,2	8,8	10,3
3	1,18	10,2	10,1

In this paper, an initial value $x = 1$ was set and convergence was reached in only 3 iterations. In Table 1 and Fig. 5 we show those iterations. The final values are $x = 1{,}18$ and $M_k = 10{,}2$ *tf.m*.

It is extremely important to check if the structure has resisted to the final obtained bending moments. To that purpose, we must have x final value less than that obtained in the bending experiment. As we have already mentioned, in this case we have got the value 1,5. This means that the pile resists well to the additional bending moments due to the measured random displacements ($x = 1{,}18 \leq 1{,}5$). In the other hand, this value of bending moment is high, considering that the Code based ultimate limit bending moment corresponds to $x = 1{,}0$. In Fig. 6 we display: M2 – bending moment about axis 3 (*tf.m*), M3 bending moment about axis 2 (*tf.m*), V2 – shear force in axis 2 direction (*tf*) and V3 – shear force in axis 3 direction (*tf*). Axis 2 and 3 are horizontal axis.

In this paper we have also taken in account the nonlinear elastoplastic behavior of the soil. We considered the soil to be linear elastic if the acting stress, computed by:

$$\sigma_i = v_i k_z \, , \tag{11}$$

is less than σ_r, given by (5) or (6). In (11), v_i is the computed displacement at node i and k_z is horizontal reaction coefficient computed at the level of node i.

Similar considerations are made for the soil stress below the pile tip. We considered the value given by (6) for the rupture stress. In this paper, for the displacements given in Fig. 1, we have stresses less than 50% of the rupture value, meaning that soil nonlinear behavior needed not to be considered, as we are well inside the linear elastic phase. In Fig. 7, we display the soil reactions upon the pile.

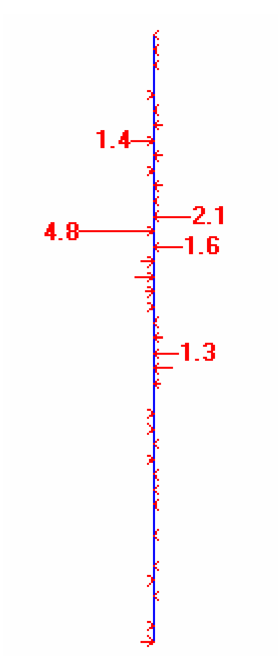

Figure 7 – Soil reactions upon the pile

4. Conclusions

We have reported here measurements of transverse displacements in piles, performed by Aoki and Alonso **[3]**. They lead to large curvature for slender piles ($L/D > 30$), due to the driving process through thick layers of soft clay. We have modeled the problem via the FEM. We have presented the effective stiffness concept of Silva and Brasil **[14, 15]** and Brasil and Silva **[9, 10]** to take in account the nonlinear behavior of reinforced concrete.

The iterative method we propose in this paper to determine the bending moments along the pile axis has converged in very few steps. Results show that resulting bending moments are considerably large, even larger than those prescribed in the Brazilian Code.

Results also show that the studied pile (D = 50 *cm*), manufactured by SCAC, resisted to the additional stresses due to transverse displacements occurred during the driving process. The welded metal connections between the concrete segments have also resisted to the prescribed design loads plus the additional bending moments due to the transverse random displacements, as verified by the 6 static loading proofs carried out in the site, without rupture for loads up to the double of the prescribed design loads.

References

1. ACI COMMITTEE 318, Building Code Requirements for Reinforced Concrete, ACI, Detroit, EUA, (1971).
2. ALONSO, U. R., Dimensionamento de Fundações Profundas, Editora Edgard Blucher Ltda., São Paulo, (1989).
3. AOKI, N. and ALONSO, U. R., Instabilidade Dinâmica na Cravação de Estacas em Solo Moles da Baixada Santista, Simpósio Sobre Depósitos Quaternários da Baixadas Litorâneas Brasileiras, ABMS-RJ, (1988).
4. ARORA, J. S., Introduction to Optimal Design, McGraw-Hill, (1989).
5. ASSOCIAÇÃO BRASILEIRA DE NORMAS TÉCNICAS – ABNT - NBR-6118, Projeto e Execução de Obras de Concreto Armado, (1978).
6. ASSOCIAÇÃO BRASILEIRA DE NORMAS TÉCNICAS – ABNT - NBR-6118, Projeto de Estruturas de Concreto - Procedimento, (2003).
7. ASSOCIAÇÃO BRASILEIRA DE NORMAS TÉCNICAS – ABNT - NBR-6122, Projeto e Execução de Fundações, (1996).
8. ASSOCIAÇÃO BRASILEIRA DE NORMAS TÉCNICAS – ABNT - NBR-8681, Ações e segurança nas estruturas, (1984).
9. BRASIL, R. M. L. R. F. and SILVA, M. A., Determination of Effective Bending Stiffness Using Optimization Techniques Applied To Experimental Results, XXV CILAMCE, Recife, Brazil, (2004).
10. BRASIL, R. M. L. R. F. and SILVA, M. A., RC Large Displacements: Optimization Applied To Experimental Results, CST, Lisbon, (2004).
11. CHAHANDE, A. I. and ARORA, J. S., Optimization of Large Structures Subjected to Dynamic Loads With the Multiplier Method, International Journal For Numerical Methods in Engineering, 37, pp. 413-430, (1994).
12. FUSCO, P. B., Estruturas de concreto - Solicitações Normais, Guanabara Dois, Rio de Janeiro, (1981).
13. SANTOS, L. M.**,** Sub-rotinas Básicas do Dimensionamento de Concreto Armado, São Paulo, Thot Editora Ltda., (1994).
14. SILVA, M. A. and BRASIL, R. M. L. R. F., Técnicas de Otimização Aplicadas a Resultados Experimentais no Estudo da Redução da Rigidez Flexional em Estruturas de Concreto Armado, Boletim Técnico da EPUSP, BT-PEF-0401, São Paulo, (2004).
15. SILVA, M. A. and BRASIL, R. M. L. R. F., Nonlinear Dynamic Analysis Based on Experimental Results of RC Towers for Telecommunication Subjected to Wind Loading, DINCON2004 - 3º Congresso Temático de Dinâmica e Controle da SBMAC, Ilha Solteira, (2004).
16. SUSSEKIND, J. C., (1979), Curso de Concreto, Editora Globo, Rio de Janeiro.

Annex 1 - Determination of effective Bending Stiffness as Function of the Bending Moment Value Based on Experimental Data and Optimization Techniques

Consider the neutral line differential equation

$$EI_{EF}(z)v(z)'' = -M_k(z), \tag{A.1}$$

where $I_{EF}(z)$, $v(z)$ e $M_k(z)$ are, respectively, the effective moment of inertia, the transverse displacement and characteristic bendin moment in a section at abscissa z. The elastic modulus of the concrete E is a function of the fck characteristic resistance, as predicted by NBR-6118-78 **[5]** Brazilian Code. In our case, boundary conditions are $v(0) = 0$ and $v'(0) = 0$.

The one-dimensional domain of the structure is the $\Delta = \{z \in \Re \mid 0 \le z \le L\}$ set. We divide Δ in n equal segments with $h = L/n$ length each. The domain of the discretized structure is now $\Delta_n = \{z \in \Re \mid z = z_0,\ z_1,\ \cdots\ z_i,\ \cdots\ z_n\}$. For each point z_i, $i > 0$, in the domain of the structure, we determine $v_i = v(z_i)$, $v'_i = v'(z_i)$ e $v''_i = v''(z_i)$ using the following integration scheme:

$$\begin{aligned} v''_i &= -\frac{M_k(z_i)}{EI_{EF}(z_i)} \\ v'_i &= v'_{i-1} + \frac{v''_i + v''_{i-1}}{2} h \\ v_i &= v_{i-1} + \frac{v'_i + v'_{i-1}}{2} h \end{aligned} \tag{A.2}$$

For each section $z_{i,}$, we consider the effective moment of inertia

$$I_{EF}(z_i) = w_i\, I(z_i), \tag{A.3}$$

where $I(z_i)$ is the moment of inertia of the integral homogeneous section z_i and w_i is the effective stiffness parameter, that is, the part of $I(z_i)$ that will effectively act for a certain bending moment value. The full section bending stiffness is defined as $EI(z_i)$, while the effective stiffness is $EI_{EF}(z_i)$. As I_{EF} depends on z_i and w_i, we will denote $I_{EF}(z_i,w_i)$. As a consequence, we have $v_i = v(z_i,\boldsymbol{w})$, with vector $\boldsymbol{w} = [w_0\ \ w_1\ \ \cdots\ \ w_i\ \ \cdots\ \ w_n]^T$.

Let us consider we have performed the experimental work described in Item 3 of this paper. Real displacements $v_r(z_i)$ are measured at some m sections of the structure under a certain loading level. The absolute quadratic approximation error between displacements given by (A.2) and those measured experimentally is the summation of the m terms:

$$E_q(\mathbf{w}) = \frac{1}{2}\sum_i [v(z_i,\mathbf{w}) - v_r(z_i)]^2 \tag{A.4}$$

We pose the following optimization problem. Determine $\boldsymbol{w} \in \Re^{n+1}$ to minimize the objective function

$$f(\boldsymbol{w}) = E_q(\boldsymbol{w}), \tag{A.5}$$

subjected to:

$$w_s(z_i) \le w_i \le 1, \quad \text{para} \quad i = 0,1,\ldots,n \tag{A.6}$$

with $w_s(z_i) = I_s(z_i)/I(z_i)$, and I_s being the moment of inertia of only the steel reinforcement. By solving the problem given by (A.5) and (A.6), we obtain the stiffness ratios $\boldsymbol{w}$ for a certain loading. Repeating the procedure for all loading cases, it is possible to establish a relationship between w_i and $M_k(z_i)/M_u(z_i)$, M_u being the ultimate limit bending moment of the section computed as prescribed by NBR-6118-03 **[6]** Brazilian Code. For the present case, we have what is displayed in Fig. A.1.

Solving the optimization problem for all load cases and sections $[M_{ki}/M_{ui}, w_i] \equiv (x_i, y_i)$ and using the following functions $y = f(x)$:

$$\begin{array}{lll} \text{(I)} & \text{Linear} & y = ax + b \\ \text{(II)} & \text{Parabolic} & y = ax^2 + bx + c \\ \text{(III)} & \text{Cubic} & y = ax^3 + bx^2 + cx + d \\ \text{(IV)} & \text{Quadric} & y = ax^4 + bx^3 + cx^2 + dx + e \\ \text{(V)} & \text{Trigonometric 1} & y = a\sin\{[(\pi/2)/0,8]x\} + b\cos\{[(\pi/2)/0,8]x\} \\ \text{(VI)} & \text{Trigonometric 2} & y = a\sin(bx) + c\cos(dx) \end{array} \tag{A.7}$$

We obtain coefficients a, b, c, d e e. For the present case, we obtain values presented in Fig. A.1 and Table A.1. We observe in this figure that as the value of the bending moment increases, the effective stiffness gets smaller. Generally speaking, any of the above functions could represent the effective stiffness. Of course, the one leading to the least approximation error for a given interval is the best choice.

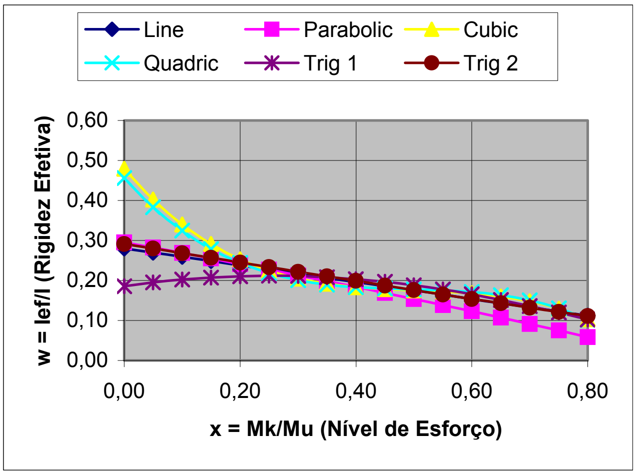

Figure A.1 – Curves for ø50 cm SCAC pile (Brasil and Silva **[9]**)

Table A.1 –Coefficients of the effective stiffness parameter (Brasil and Silva **[9]**)

Equation	Coefficients - Design Variables					Obj. Func.	Lagrag.
	a	b	c	d	e	App. Error	Iterations
Line	-0,209974	0,279928	-	-	-	0,41	23
Parabolic	-0,041644	-0,262344	0,295252	-	-	0,36	7
Cubic	-2,136078	3,235075	-1,690812	0,478874	-	1,00	8
Quadric	-0,028670	-2,122856	3,176175	-1,610085	0,455779	1,19	10
Trig 1	0,102035	0,185791	-	-	-	1,75	4
Trig 2	-0,306448	0,753699	0,291575	0,271006		0,39	8

Brasil and Silva **[9]** found that the cubic function is the best fit for the effective stiffness parameter w inside the $0 \leq x \leq 0.8$ interval. The same experimental procedures have also shown that the sample pile broke with $x = 1.5$, that is, it resisted 50 % more than the ultimate moment predicted by NBR-6118-03 **[6]** Brazilian Code. For values of x above 0.8, the authors concluded that the straight line given in Brasil and Silva **[9]** is a better fit.